Optica Applicata, Vol. XLIII, No. 3, 2013
DOI: 10.5277/oa130302

Evaluation of road signs using radiometric and geometric data from terrestrial LiDAR

Higinio GONZÁLEZ-JORGE*, Belén RIVEIRO, Julia ARMESTO, Pedro ARIAS

Department of Natural Resources and Environmental Engineering,
School of Mining Engineering, University of Vigo, Spain

*Corresponding author: higiniog@uvigo.es

Maintenance works are crucial to reduce the risk of accidents. Road signs appear to be one of the most important elements for safety purposes so their inspection is commonly included in the most extended road management systems. The geometric state of the sign is of great importance, especially interesting is its flatness and the inclination relative to the ground. Road signs are printed with reflective paints to maximize the visibility to the drivers. This coating produces a high reflected radiation that is easily recorded by the photoelectric detector of the laser scanner mechanisms. It allows establishing an intensity based filter in order to perform the 3D classification of the road sign.

In this work, a number of road signs are evaluated, under a geometric point of view, using the laser scanner Riegl LMS Z390i. A Matlab algorithm is developed for all the data processing (3D classification and evaluation of geometric parameters). Results do not show the evidence of folded or abnormally tilted signs. The developed algorithms open the possibility of using the attribute of intensity of laser scanning data for classification purposes, during the automatic evaluation of the condition state of road signs. Such algorithms could increase the productivity and reliability of the inspection works.

Keywords: road inspection, laser scanning, radiance, road sign.

1. Introduction

Safety on the roads has become an issue of vital importance, social concern and widespread media coverage in our days. The risks for the users are mainly reduced by implementing three complementary strategies. The first is related to the road design and maintenance; the second one to the vehicle safety; and the third strategy is associated with the regulations pertaining to the road users. Proper maintenance is a key factor for the safety of drivers due to the roads deterioration over time [1, 2]. The main reasons of deterioration are primarily due to accumulated damage from vehicles, as well as the environmental effects (*i.e.*, frost heaves, thermal cracking, oxidation). Maintenance programs are normally conducted by three basic stages: *i*) inspection of the road; *ii*) evaluation of the condition state; and *iii*) decision-making and intervention if necessary. The rehabilitation works include treatments for fixing asphalt concrete (*i.e.*, crack sealing, micro-milling and surface treatments), slab stabilization, joint sealing, re-draw of line markings, and replacement of damaged traffic signs.

During the last years, high-performance vehicles are more and more used for the automated inspection of the roads. Such vehicles can include several geoscience sensors:

– Profilers which provide the measure of the international roughness index (IRI), the ride number (RN), rut depth and macro texture;

– Friction testers that provide the continuous coefficient of friction;

– Road surface deflectometers which are used for the evaluation of the structural response of the pavement;

– Ground penetrating radar systems that allow pavement thickness to be estimated;

– Laser scanners that acquire data of transverse profiles across the road longitudinal direction, bridge heights and vertical and horizontal clearances, digital terrain models, tunnel survey and ground movement monitoring [3].

Laser scanners are ideally suited for mobile surveying and mapping applications. They provide a large amount of data in a very short period of time. These systems typically operate in conjunction with digital video cameras, that allows colored point clouds to be collected. However, this technology makes the development of technical procedures and algorithms for data processing necessary in order to automatically obtain the required information from the road.

Laser scanning systems typically provide geometric and radiometric information, in addition to that recorded by the associated cameras. The power of the reflected radiation that reaches the photodetector of the scanner, usually known as an attribute of intensity, depends on several aspects such as the distance to the object, wavelength, environmental conditions, incidence angle on the object, and the own reflectance of the surface [4].

This technical note shows a procedure to automatically evaluate the condition state of the road signs using the radiometric and geometric information obtained by a laser scanner system. Radiometric data, defined by the attribute of intensity, are used for classification purposes and geometric data for the determination of their condition state.

2. Laser scanner fundamentals

Non-contact techniques for surveying infrastructure components have evolved significantly in the last decade, making possible the capture of dense point clouds with image information for 3D modeling and extraction of features. Terrestrial laser scanning systems are usually classified according to the method used for laser ranging. Two main methods are: time-of-flight by a pulsed laser and phase shift scanners [5–8].

Scanners based on time of flight principles emit a short light pulse, which, after reflection by the target surface, is focused by the photodetector. The distance is evaluated by measuring the time delay of the laser pulse traveling between the point of emission and the surface being scanned. The range r is calculated as:

$$r = 0.5c\Delta t \quad (1)$$

where c is the speed of light, and Δt is the time delay of the pulse.

Scanners based on phase shift measurements ($\Delta\varphi$) use a continuous laser wave as a carrier for a modulated signal. The phases of the emitted and received signals are compared and related with the range measurement:

$$r = \frac{\Delta\varphi}{2\pi}\frac{\lambda}{2} + \frac{\lambda}{2}n \tag{2}$$

where λ is the wavelength of the modulated wave and n is the unknown number of full wavelengths between the sensor system and the reflecting object. Scanners of this type have a lower range, higher measurement rate and usually better precision than scanners based on the principle of time of flight.

Terrestrial laser scanners can collect data in two different modes, static and mobile. The first mode collets 3D data centered into a spherical coordinate system from its surrounding environment. Mobile terrestrial laser scanners combine a positioning system with a 2D laser scanner. 3D data are built by fanning out the 2D data of the scanner along the vehicle trajectory. The positioning system integrates global navigation satellite systems (GNSS) for position estimation, inertial navigation systems (INS) for attitude evaluation and distance measurement indicators (DMI) for distance calculation. All this information is processed using a Kalman filter algorithm [9] to calculate the trajectory of the mobile system. The presence of INS/DMI is necessary to fully complement the GNSS information in locations without satellite coverage (*i.e.*, in tunnels, under bridges, on road slopes, and on roads between canyons or dense tree canopies) [10, 11].

Analogously to digital RGB cameras, which record light in the visible spectrum (approximately 400–700 nm) onto a digital CCD/CMOS sensor (where a digital value is associated with each pixel), laser scanners record a measurement of the returning laser beam power, as well as the range and angular measurements. This measurement is referred to as the “intensity” or reflectance value, and it corresponds to a fraction of the emitted laser power.

Typically, this value is normalized in the range of 0 to 1 or 0 to 255, although how it is computed is not revealed by laser manufacturers. The resolution of the system depends on the electronics of the laser. For example, an 8-bit converter makes it possible to obtain 256 levels (0.04 step size in the 0–1 range) and a 10-bit converter yields 1024 levels (0.00098 step size in the 0–1 range).

According to the principles of interaction between electromagnetic radiation and matter, usually expressed by the radar range equation [12], the intensity or reflectance values directly depend on the physical characteristics of the material (*i.e.*, roughness of the surface), the wavelength of the incident radiation, and the distance between the laser and the object [13]

$$I = \frac{\rho\cos(\alpha)}{r^2\mu C} \tag{3}$$

where ρ is the target reflectivity, α – the angle of incidence, r – the range to the target, μ – the transmission factor and C – an unknown constant.

3. Materials and methods

3.1. Terrestrial laser scanner RIEGL LMS Z-390i

A terrestrial laser scanner manufactured by RIEGL, model LMS-Z390i, was used in this work. This instrument is composed of an accurate and fast 3D scanner with the associated software RISCAN PRO. The RIEGL LMS-Z390i (Fig. 1) is a rugged and fully portable sensor especially designed for the rapid and accurate acquisition of high-quality 3D images and specifically rated for long range measurements as architecture and *façade* measurement, archaeology and cultural heritage documentation, civil engineering, city modeling, and surveying.

Fig. 1. RIEGL LMS Z390i during surveying process.

Measurements are performed using the time of flight principle for range and two encoders for angular evaluation. Precision mechatronics systems are used for positioning the mirrors which orientate the laser beam to the measuring field. A rotating mirror with 90° travel is used for vertical beam deflection and a servo motor that rotates 360° around the vertical axis of the instrument allows the horizontal scanning. The point cloud obtained in spherical coordinates (R, θ, ϕ) is then directly converted into

Table 1. Technical specifications of laser scanner RIEGL LMS Z390i.

Measurement range	< 400 m
Minimum range	> 1 m
Accuracy (50 m)	6 mm
Repeatability (50 m)	4 mm
Measurement rate	11.000 Hz
Laser wavelength	1.540 nm
Beam divergence	0.3 mrd
Vertical scanner range	80°
Horizontal scanner range	360°
Vertical and horizontal step-width	0.002°

Cartesian coordinates (X, Y, Z) by the software. Furthermore, the laser scanner used in this experiment includes an infrared class 1 laser, which means that it is inherently safe and that there is no possibility of eye damage. Technical characteristics of the instrument are shown in Table 1.

3.2. Area of study

The Rías Baixas A-52 is a highway between the towns of Benavente (Zamora) and O Porriño (Pontevedra), both located in northwest Spain. It is 306 km long and connects the provinces of Pontevedra, Ourense and Zamora with Madrid. Construction began in 1994 and was completed in 1998. The work proved to be more costly than initially estimated due to the complex orography of the Ourense and Pontevedra provinces, as well as the frequent occurrences of landslides and terrain instability. The connection between the city center of Ourense (N-120) and A-52 is particularly

Fig. 2. Connection between the Rías Baixas A-52 and the city center of Ourense.

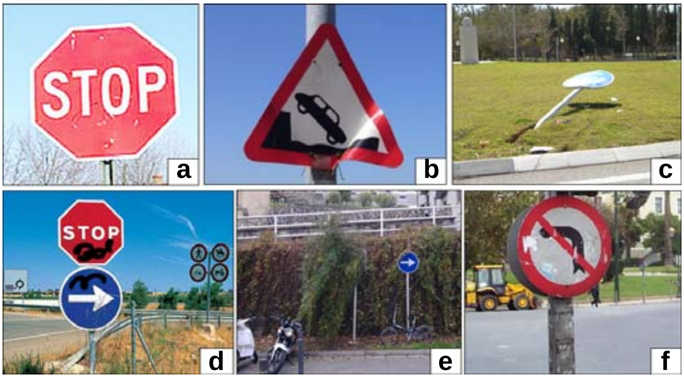

Fig. 3. Different examples of damages in traffic signs: paint deterioration (**a**), folded sheet (**b**), pole bent (**c**), vandalism (**d**), concealment by vegetation (**e**) and adhered substances (**f**).

dangerous because of its location in mountainous terrain and along a river. Therefore, the speed and maneuverability are limited and enforced by a high density of traffic signs (Fig. 2).

Traffic signs degrade over time from dirt substances, wind storms, vandalism, water damage, vegetative growth, and vehicle collisions. Consequently, degraded signs lose the ability to help drivers navigate safely. Figure 3 shows some examples of different traffics signs and their associated damages.

3.3. Data acquisition and processing

Data acquisition is performed from a roundabout that is located at the highway entrance (Fig. 1). The scanner is leveled using a tribrach on a topographic tripod. The traffic was not interrupted. First, a low resolution panoramic scan (overview) is made all around the full field of view (360 °) of the horizontal angle range and 0.2° step-width (Fig. 4**a**). The scan has 713216 points and takes around 1 minute for the acquisition. Once all the objects are situated, the highway entrance is scanned in detail (Fig. 4**b**). Scan acquisition characteristics are a step-width of 0.04°, 1986892 measured points and around 8 minutes of time.

The non-interruption of the traffic increases the productivity of the method and does not cause discomfort to the traffic authorities or drivers. However, this causes the return echoes that do not represent any part of the road. The echoes appear as a vertical set of points that come from the vertical movement of the mirror of the scanner, which is faster than the horizontal movement. Typically, no more than two or three vertical set lines of points appear for each vehicle, because the traffic is not congested. These anomalous points were cleaned using filtering algorithms implemented into the RISCAN PRO software (RIEGL) (Fig. 5).

The next step into the processing consists in the automatic classification of the traffic signs in order to subsequently evaluate their condition state. The RIEGL scanner assigns radiance values ranging from 0.0 to 1.0 to each of the coordinates of the point

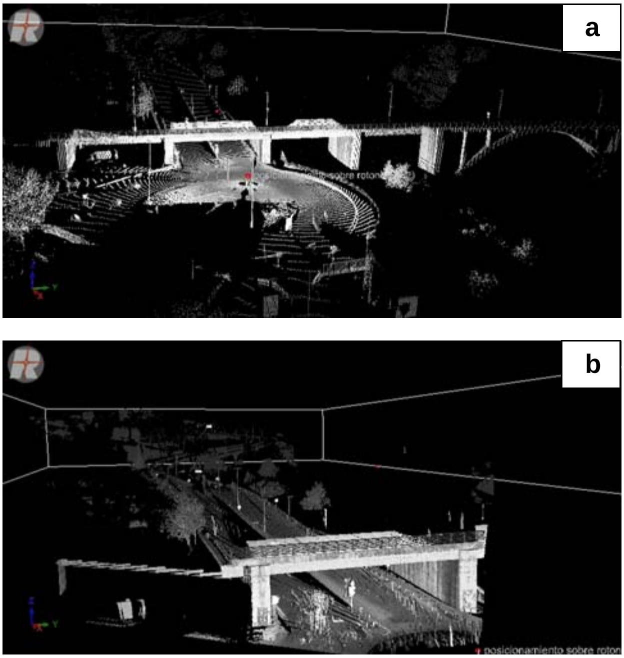

Fig. 4. Overview (**a**) and detailed (**b**) scan.

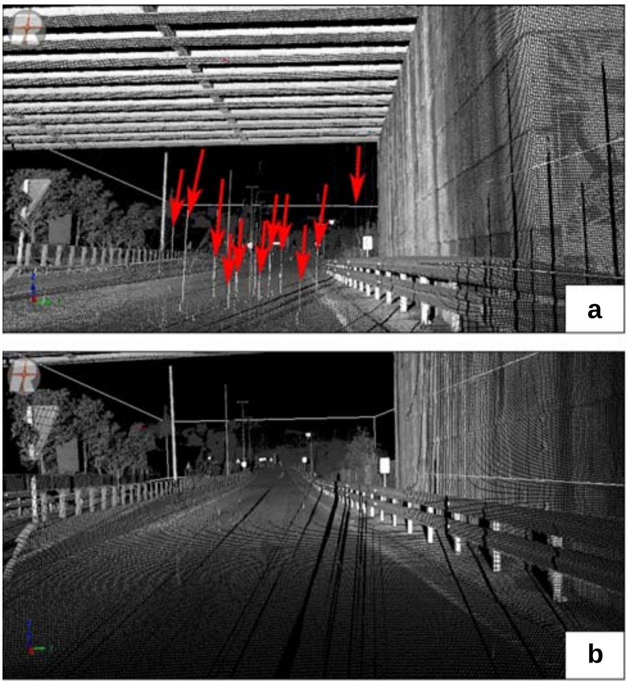

Fig. 5. Echoes from vehicles (**a**) and point cloud filtered using the disconnected points filter (**b**).

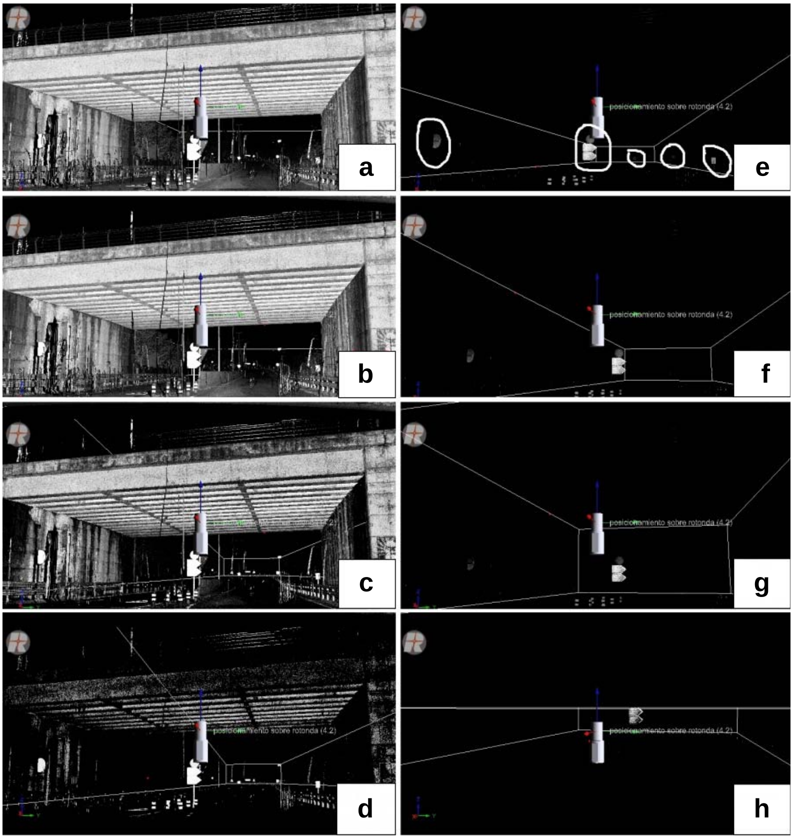

Fig. 6. Calibration of the radiance threshold: 0.0–1.0 (**a**), 0.1–1.0 (**b**), 0.2–1.0 (**c**), 0.3–1.0 (**d**), 0.4–1.0 (**e**), 0.5–1.0 (**f**), 0.6–1.0 (**g**) and 0.7–1.0 (**h**).

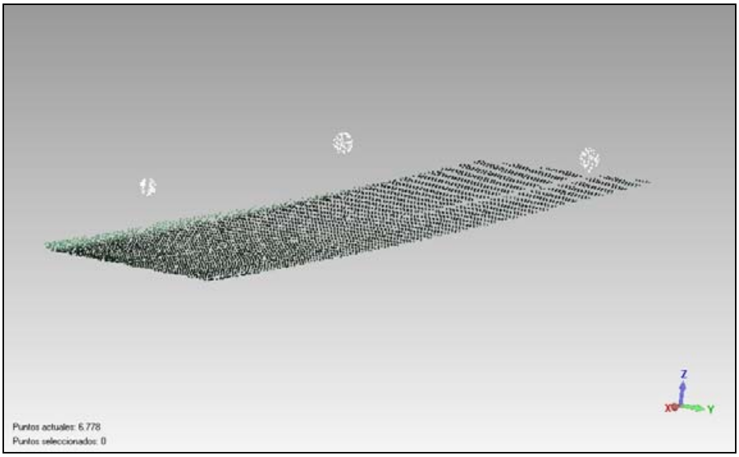

Fig. 7. Merged point cloud including traffic signs and pavement.

cloud, using an 8 bit converter. This radiance value is widely named by the term "intensity" and denotes a portion of the power of the emitted radiation. According to this, a value of 1.0 means that the radiation emitted by the laser diode is equal to that which reaches the photodetector. The classification process can only be properly made by the calibration of the appropriate threshold. This process can be seen in Fig. 6. The results show that values between 0.4 and 1.0 (Fig. 6**e** – see highlighted) extract all the information related to the signs and avoid the other elements of the road (*i.e.*, pavement, vegetation, guardrails, light poles). Taking this into account, the intensity interval between 0.4 and 1.0 is used for the classification purposes.

Figure 7 shows another example of some traffic signs automatically segmented from this survey using the intensity threshold. A layer referred to the pavement is merged with the signal data to make it more understandable. Pavement classification is made manually from the point cloud. All the signs are correctly segmented (100% of true values). The method is robust against other road elements that could enter confusing information. For example, a pole used for lighting purposes does not depict the high reflectivity to the laser light that is depicted by the paintings of the traffic signs. On the other hand, the license of a car always appear inside the limits of the road pavement and the ground height is smaller than that presented for a traffic sign, so the differentiation is clear.

Finally, the flatness of each sign is automatically evaluated using the least squares fitting algorithm for the front face of signs and by calculating the standard deviation of identified front face planes. As expected, the calculated change in standard deviation demonstrates the ability to automatically identify bent or warped signs, and may be implemented for physical condition inspections. Least square fitting calculates the coefficients of a fitting plane (a, b, c) which minimizes the function

$$f(a, b, c) = \sum_{i=1}^{n} (ax_i + by_i + c - z_i) \tag{4}$$

being x_i, y_i and z_i the point coordinates of the sign. Standard deviation is evaluated by

$$\sigma = \sqrt{\frac{1}{N}\sum_{i=1}^{N} (ax_i + by_i + c - z_i)^2} \tag{5}$$

where N is the number of data points.

This algorithm is tested in the laboratory, previously to the processing of the field data. Laboratory test consists of the comparison of two different scans (Fig. 8). First scan is performed using a sign in perfect condition state. Second scan is made artificially folding the sign. Differences in the standard deviation change from 0.003 to 0.018 m. This change demonstrates, as must be expected, that a folded sign increases the standard deviation of the plane and can be used for alert purposes during road inspections.

In addition, the angle between the normal vector of the fitted plane and the Z direction of the surveying is also calculated. The laser scanner was leveled and the signs should

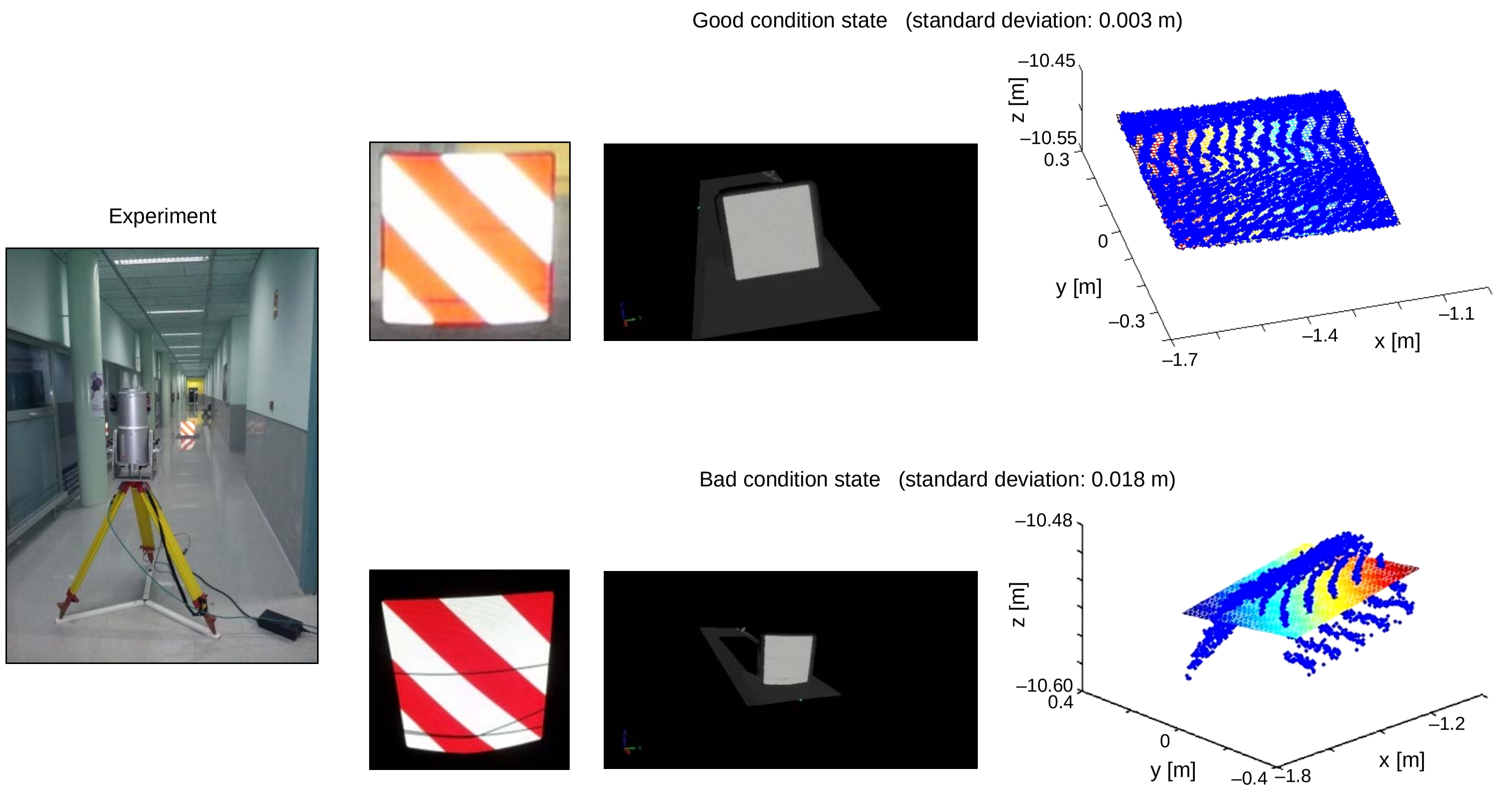

Fig. 8. Summary of the process to automatically inspect folded signs.

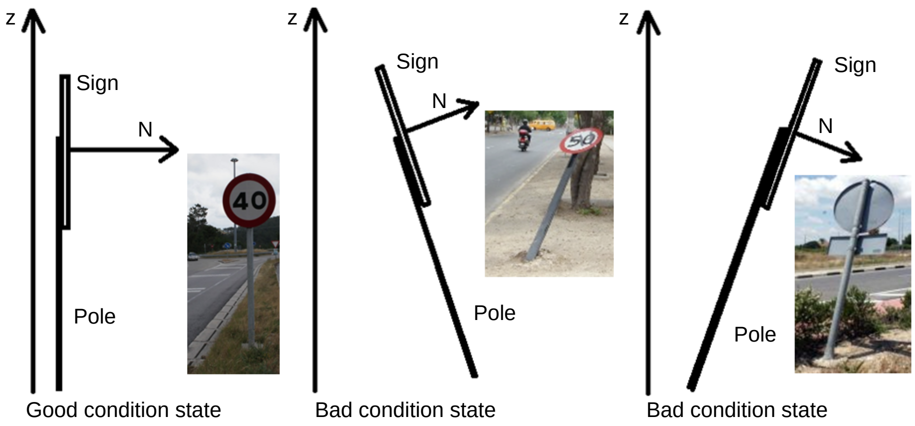

Fig. 9. Summary of the process to automatically evaluate abnormally tilted signs.

be perpendicular to the ground, so a sign in good condition state must show an angle around 90°. An important change in this angle could be a symptom of deterioration caused by vandalism, vehicular collision or strong winds (Fig. 9).

4. Results and discussion

A total of 16 signs were automatically segmented from the point cloud for this study. The standard deviation of the fitted plane and the angle of the normal vector with the Z axis are exhibited in Table 2. Threshold values are selected in the software to alert abnormal geometries in the signs. Such thresholds are 0.008 m for the standard deviation and $90° \pm 5°$ for the angle between the sign normal vector and the Z axis. First value is selected from the technical specifications of the scanner (Table 1), which show a repeatability of 0.004 m for 1σ Gaussian probability distribution; 2σ is considered for this case to cover other error sources. According to a Gaussian distribution, 2σ value covers approximately the 95% of the data. The second threshold comes from the recommendation of experts in road maintenance, who are in close

T a b l e 2. Summary of the results; α – angle between the normal vector of the sign plane and the Z axis and std – the standard deviation of the plane fitted to the sign data.

Sign number	α [°]	Std [m]	Sign number	α [°]	Std [m]
1	90.1	0.003	9	91.7	0.004
2	89.1	0.002	10	90.3	0.003
3	91.3	0.003	11	90.8	0.002
4	90.7	0.003	12	89.3	0.004
5	91.5	0.001	13	91.3	0.002
6	89.8	0.004	14	89.9	0.002
7	89.4	0.001	15	90.3	0.003
8	91.3	0.003	16	90.1	0.001

collaboration with our research group, and consider that values around 90° ± 5° allow good visibility for the drivers.

All the signs under study do not present important deviations in the standard deviation of the fitted plane or the normal vector, so no evidence of damages from vandalism, vehicular collision or extreme weather conditions can be determined. Taking into account the results, no maintenance works must be done for these signs.

5. Conclusions

This work is a contribution to the automation, the systematization and the establishment of rules for the tasks concerning road inspection programs. The advantage of the method proposed is that a direct geometry of the sign can be recorded and used to obtain quantitative measurements. Quantitative information can be saved into the databases of road management systems and contribute to the decision making. Therefore, rehabilitation works in the infrastructure can be correctly and accurately planned ensuring the safety of the road users and saving economic costs. In addition, the technique can be automatized in order to increase productivity during the road inspections.

The procedure developed for this work uses the data obtained from a terrestrial laser scanner to automatically evaluate some important parameters for determining the condition state of the traffic signs. The results are obtained from a static system, although they can be easily extrapolated to a mobile unit, with higher productivity and lower labor costs. The optical characteristics (*i.e.*, wavelength) of most static and mobile time of flight scanners are similar, so the results can be easily transferred.

The procedure is essentially based on the classification of the geometry of the signs based on their intensity values. The sign status is evaluated using two different parameters which are also automatically calculated. The first parameter is based on the standard deviation of the fitted plane to the sign, and the second one on the determination angle between the normal vector of the fitted plane and the vertical direction. No abnormal geometries are detected for all the signs under study. Future research must include the evaluation of damaged or deficient signs with field measurements.

The methodology described in this technical note can be easily transferred to other tasks related to the inspection of horizontal signalization, since the high reflectivity of the painting would allow easy classification of the elements. Another possible application is connected with the condition state of the guardrails which use reflective markers to improve the night vision of the drivers. Those reflective markers are also good laser reflectors that could be easily used for quick guardrail classification.

Acknowledgements – Authors give thanks to the financial support of the Spanish Ministry of Science and Education (Grant No. BIA2009-08012), the Spanish Centre for Technological and Industrial Development (Grant No. IDI-20101770) and for the grant for Human Resources IPP055 – EXP44 from Xunta de Galicia. Authors also thank the companies Extraco Construcciones y Proyectos SA, Misturas Obras y Proyectos SL, Enmacosa SA, Ingeniería Insitu SL y Logica SA for their helpful collaboration.

References

[1] VERA I., THENOUX G., SOLMINIHAX H.D., ECHAVEGUREN T., *Technical assessment model for the performance of flexible pavement maintenance*, Revista de la Construcción **9**(2), 2010, pp. 76–88.

[2] PELLEGRINO C., PIPINATO A., MODENA C., *A simplified management procedure for bridge network maintenance*, Structure and Infraestructure Engineering **7**(5), 2011, pp. 341–351.

[3] FINDLEY D.J., CUNNINGHAM C.M., HUMMER J.E., *Comparison of mobile and manual collection for roadway components*, Transportation Research **19**(3), 2011, pp. 521–540.

[4] ARMESTO-GONZÁLEZ J., RIVEIRO-RODRIGUEZ B., GONZÁLEZ-AGUILERA D., RIVAS-BREA M.T., *Terrestrial laser scanning intensity data applied to damage detection for historical buildings*, Journal of Archaeological Science **37**(12), 2010, pp. 3027–3047.

[5] PFEIFER N., BRIESE C., *Laser scanning: principles and applications*, 3rd International Exhibition and Scientific Congress on Geodesy, Mapping, Geology, Geophysics, Novosibirsk, Russia, 2007.

[6] RUEGER J.M., *Electronic Distance Measurements*, Springer, Berlin, 1990.

[7] WEHR A., LOHR U., *Airborne laser scanning – An introduction and overview*, ISPRS Journal of Photogrammetry and Remote Sensing **54**, 1999, pp. 68–82.

[8] GONZÁLEZ-JORGE H., RIVEIRO B., ARMESTO J., ARIAS P., *Standard artifact for the geometric verification of terrestrial laser scanning systems*, Optics and Laser Technology **43**(7), 2011, pp. 1249–1256.

[9] TITTERTON D., WESTON J., *Strapdown Intertial Navigation Technology*, 2nd Ed., Institution of Engineering and Technology, Stevenage, UK.

[10] LEVY L.J., *The Kalman Filter: navigation's Integration Workhorse*, GPS World, September 1997, pp. 65–71.

[11] KAVANAGH M., *Gyroscopes for orientation and inertial navigation systems*, Kartografia i Geoinformacije **6**, 2007, pp. 254–271.

[12] HÖFLE B., PFEIFER N., *Correction of laser scanning intensity data: Data and model-driven approaches*, ISPRS Journal of Photogrammetry and Remote Sensing **62**, 2007, pp. 415–433.

[13] LILLESAND T.M., *Remote Sensing and Image Interpretation*, 5th Ed., Wiley, India, 2009, p. 820.

Received November 17, 2012
in revised form December 20, 2012